

The Hurricane Imaging Radiometer – An Octave Bandwidth Synthetic Thinned Array Radiometer

Christopher Ruf¹, Ruba Amarin², M.C. Bailey³, Boon Lim¹, Robbie Hood⁴, Mark James⁴, James Johnson², Linwood Jones², Vanessa Rohwedder⁴ and Karen Stephens⁴

1. Space Physics Research Laboratory, AOSS Dept., University of Michigan

2. Central Florida Remote Sensing Lab, ECE Dept., University of Central Florida

3. RTI International, Hampton, VA

4. National Space Science & Technology Center, NASA Marshall Space Flight Center

Abstract—The Hurricane Imaging Radiometer (HIRad) is a new airborne sensor that is currently under development. It is intended to produce wide-swath images of ocean surface wind speed and near surface rain rate in hurricane conditions. HIRad will extend the scientific capabilities and technologies associated with two previous successful airborne microwave radiometers: the real aperture Stepped Frequency Microwave Radiometer (SFMR) and the synthetic aperture Lightweight Rainfall Radiometer (LRR). Both SFMR and HIRad are required to operate over the full C-Band octave in order to estimate precipitation levels experienced in hurricanes without saturation and to penetrate through the precipitation and estimate surface winds. Operation over an octave bandwidth was easily accomplished by the nadir-pointing horn antenna used by SFMR. However, it represents a major technological challenge for the HIRad design because it is a Fourier synthesis imager. Details of how HIRad meets that challenge are described here.

Keywords—microwave radiometry, synthetic aperture radiometry, ocean remote sensing

I. INTRODUCTION

The Hurricane Imaging Radiometer (HIRad) is currently under development by NASA Marshall Space Flight Center, the University of Central Florida, RTI International, and the University of Michigan. HIRad is a hybrid instrument design, based on the Stepped Frequency Microwave Radiometer (SFMR) and the Lightweight Rainfall Radiometer (LRR). SFMR is a real aperture instrument that operates at a number of distinct frequencies covering roughly the full C-Band octave. It is deployed on NOAA Hurricane Research Division aircraft to provide simultaneous real time estimates of ocean surface wind speed and rain rate [1]. SFMR has a single nadir-pointing horn antenna and makes wind and rain estimates directly below the aircraft. The Lightweight Rainfall Radiometer (LRR) is a NASA/U-Michigan airborne synthetic thinned aperture radiometer that operates at a single X-Band frequency [2, 3]. It is a cross-track imager which uses Fourier synthesis software beam forming [4]. LRR is capable of estimating either rain rate or wind speed, but not both because of its single frequency of operation. It is also limited to retrievals only in light to moderate rain rates because of its operation at X-Band [5]. SFMR, on the other hand, is able to retrieve rain rate and underlying ocean surface wind speed in severe, hurricane-strength, conditions because of its lower frequency of operation. The HIRad design combines the best

features of SFMR and LRR. It will widen the restricted, nadir-only, coverage of SFMR to a cross-track field of view of $\pm 61^\circ$ and it will expand LRR's limited dynamic range of precipitation levels to include those experienced in hurricane rain bands [6].

The key to HIRad's improved performance is its ability to operate as a Fourier synthesis imager at discrete frequencies that cover the same C-Band octave as does SFMR. Fourier synthesis imagers such as LRR are designed to work at single narrow band frequencies. Expanding the frequency coverage represents several design challenges. The HIRad antenna array is comprised of linear arrays of multi-resonant stacked microstrip patch antennas. The linear arrays produce a real-aperture fan beam antenna pattern that defines the instantaneous field of view of the sensor. The fan beam antennas are themselves configured in a thinned linear array. A synthetic-aperture pencil beam antenna pattern is formed in software from the cross-correlation products of all pairs of fan beam antennas. For a Fourier synthesis imager operating at a single frequency, the unit spacing of the thinned linear array of fan beam antennas is approximately one-half the RF wavelength ($\lambda/2$). For HIRad, however, the unit spacing must accommodate the full octave bandwidth. A spacing of less than $\lambda/2$ will degrade the spatial resolution of the imager and can create physical packing problems. A spacing of greater than $\lambda/2$ will limit the portion of the fan beam pattern that can be imaged without grating lobes appearing in the synthesized beam pattern. A compromise unit spacing is selected for HIRad that is slightly greater than $\lambda/2$ at the highest frequency and less than $\lambda/2$ at the lowest frequency. The correlating receivers used by HIRad must also be able to operate over an octave bandwidth. For a real aperture radiometer such as SFMR, operation over an octave can be readily achieved using a stepped local oscillator and double sideband down conversion. However, the correlating receivers that are used by a Fourier synthesis imager must operate with single sideband down conversion in order to preserve both quadrature components of the correlation product. The combination of octave bandwidth operation and single sideband down conversion is a challenging requirement that resulted in a different approach to the design of the receiver.

In the following sections, the HIRad system architecture and the antenna and receiver designs are described, followed by

analysis of the synthesized antenna pattern, beam efficiency, and alias-free field of view to be expected at each discrete frequency of operation.

II. SYSTEM ARCHITECTURE

HIRad needs to cover roughly the full C-Band octave in order to replicate the geophysical retrieval capabilities of SFMR. Whereas SFMR could use a single wide-band horn antenna, with frequency selection made by a variable (stepped) local oscillator, HIRad requires a planar antenna array to perform interferometric aperture synthesis. Custom multi-resonant stacked patch antennas have been designed for this purpose. The patches are resonant at the discrete frequencies of 4, 5, 6 and 7 GHz. A more detailed description of the antenna design is given in Section III. The HIRad system architecture at each discrete frequency follows a design similar to that used by the previous X-Band Lightweight Rainfall Radiometer [2]. The planar antenna array is thinned in one dimension so that 10 linear arrays are cross-correlated to synthesize a filled aperture made up of 37 linear arrays [7]. The signals from each of the 10 linear arrays are filtered, amplified, demodulated and digitized by dedicated receivers (described in Section IV). The signals are then passed to a signal processing subsystem that performs several functions. A bank of digital polyphase filters first divides the full signal passband into 16 subbands. The kurtosis of the signal in each subband is computed and recorded. The kurtosis has been found to be an excellent detector of the presence of Radio Frequency Interference (RFI) [8]. Frequency subbands found to contain RFI are excluded from subsequent processing. Common subbands from all possible pairs of the 10 signals are then cross-correlated using complex multipliers to form the raw, uncalibrated, visibility samples that make up the Level 0 archival data produced by the sensor.

The raw visibility samples are calibrated using internal reference loads, active cold loads (ColdFETs), and correlated noise diodes. Calibrated visibilities are converted to an image of brightness temperature (T_B) by a least squares inversion of the individual interference patterns that are produced by the cross-correlation of each pair of antenna elements. HIRad is a 1-dimensional synthesis push broom imager. Each of the ten linear array antenna elements has a coincident fan beam antenna pattern that is aligned on the aircraft cross-track to the direction of motion. The length of the fan beam defines the along-track angular resolution of the imager. Cross-track resolution is set by the maximum spacing between linear arrays. Individual pixels in the cross-track direction are formed in software by the least squares inversion algorithm. All cross-track pixels are produced simultaneously. Pixels are formed along track by the forward motion of the aircraft. They are produced sequentially in time.

HIRad system design parameters and performance characteristics are given in Table 1 for each of its four discrete operating frequencies. An aircraft at 11 km altitude with an air speed of 200 m/s (390 knots) is assumed. The overall

Table 1. HIRad System Design and Performance				
freq (GHz)	4	5	6	7
altitude (km)	11			
integration time (s) (20% footprint smear)	1.20			
cross track interelement spacing (m) @ 0.9"	0.023			
cross track interelement spacing (λ)	0.31	0.38	0.46	0.53
# of active array elements and correlating receivers	10			
# of synthesized baselines	36			
along track interelement spacing (m) @ 1.5"	0.038			
# of along track elements	16			
bandwidth (MHz)	85	60	60	100
Spatial Resolution				
Nadir (deg) (geom. mean of princ. planes)	7.0	5.6	4.6	4.0
Nadir (km)	1.4	1.2	1.0	0.9
30 deg cross track off-nadir (km)	1.9	1.5	1.3	1.1
60 deg cross track off-nadir (km)	5.6	4.5	3.8	3.3
Brightness Temperature Precision				
NEAT (K) (w/ 290K scene brightness)	0.19	0.25	0.27	0.22

synthesized antenna aperture size is 82x61 cm. The imaging coverage in the cross-track direction is $\pm 61^\circ$ from nadir. This corresponds to a 40 km wide swath, centered on the ground track of the aircraft. Spatial resolution will vary inversely with frequency. At nadir, the resolution varies from 0.9 to 1.4 km over 7-4 GHz. At 60° from nadir, the synthesized footprint will widen to a resolution of 3.3-5.6 km. The radiometric uncertainty in measurements of the brightness temperature (NEAT) will be 0.2-0.3 K at the finest spatial resolution. This is more than adequate to produce rain rate and wind speed estimates at levels of uncertainty as good as (if not better than) SFMR.

III. ANTENNA DESIGN

One significant design challenge with HIRad, relative to previous spatial interferometers, is the need for a planar array that covers roughly a full octave bandwidth. The HIRad antenna is a planar array of 39x18 multi-resonant stacked microstrip patch antenna elements. Each stacked patch unit consists of four rectangular metal patches interleaved between dielectric layers. The individual patches are reactively coupled to a common coaxial feed line, which enters behind a bottom ground plane. The electrically coupled system of patches is designed to be resonant at each of the target operating frequencies (4, 5, 6 and 7 GHz). An edge view of

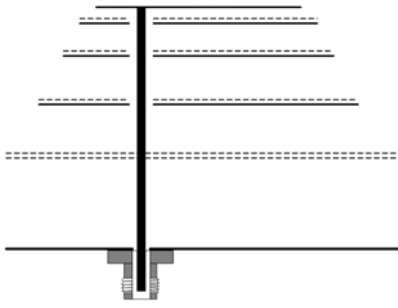


Figure 1. Edge view of HIRad multi-resonant stacked patch antenna array element. The top patch is resonant at 7 GHz, the second one at 6 GHz, etc. Strong reactive coupling between layers must be accounted for in the design to produce the desired resonant frequencies.

the stacked patch is shown in Figure 1. Different elements of the planar array serve three different functions. Ten 16-element lines of elements are coupled together by a corporate 16:1 combiner to produce the active linear arrays to which the HIRad receivers are connected. These elements are highlighted in blue in Figure 2. The 16-element lines of elements between them, as well as a perimeter of elements that runs around the outer edge of the planar array, are all terminated with impedance matched loads. They allow for each active array element to “see” a reasonable approximation of an infinite array around it for purposes of uniformity in impedance matching.

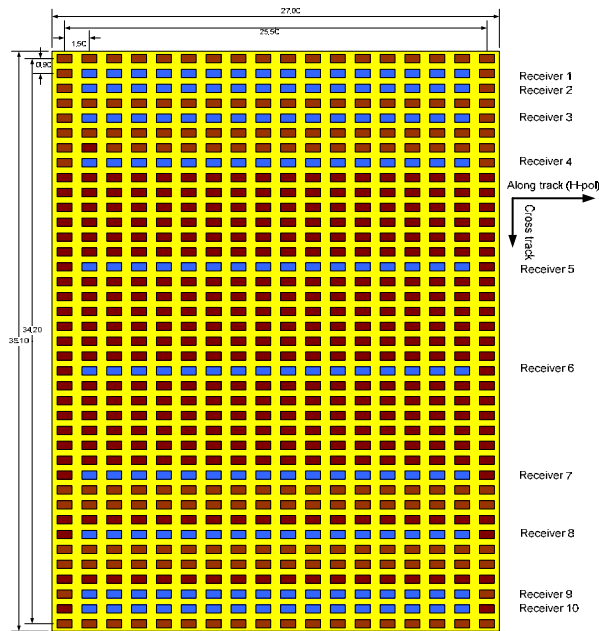


Figure 2. Layout of HIRad planar array. The ten active 16-element linear arrays are shown in blue. Passive 16-element linear arrays between them, as well as an outer perimeter of elements, are all match loaded. This stabilizes the mutual coupling, input impedance and radiation patterns of the active elements.

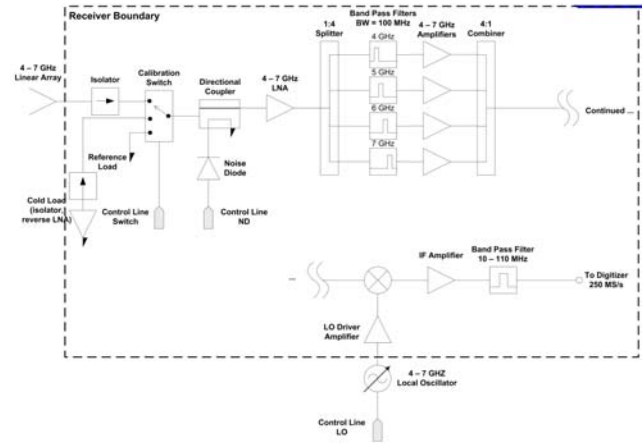


Figure 3. HIRad correlating receiver functional block diagram. Each of the ten active linear arrays is connected to one of these receivers. Individual receiver gain and offset are calibrated using internal ambient reference loads and active cold load reversed LNA “ColdFETs”. Correlated gain is calibrated using a single noise diode that is split ten ways and distributed to each receiver. Single sideband down conversion is achieved using image rejection bandpass filters centered to the four resonant frequencies of the patch antennas.

IV. RECEIVER DESIGN

A second design challenge is the need for HIRad’s correlating receivers to also cover roughly a full octave bandwidth. A block diagram of one receiver is shown in Figure 3. Frequency down conversion is needed to move the signal passband to an IF that is compatible with the receiver’s digitizer. For spatial interferometry applications, the down conversion must be single sideband. This is accomplished using a parallel filter bank at the RF stage. Each of the four bandpass filters is centered at one of HIRad’s operating frequencies and is narrow enough to reject the adjacent image sideband during down conversion. Once the unwanted sideband has been filtered out, a standard double sideband mixer can be used, similar to the SFMR hardware approach.

V. IMAGING PERFORMANCE

HIRad’s near-octave frequency coverage necessitates an inter-element spacing between antenna array elements at 7 GHz that is greater than $\lambda/2$. The impact of this on the field of view of the imager was assessed by examining the beam efficiency of the synthesized antenna pattern as a function of off-nadir scan angle. A theoretical model was used to estimate the antenna interference patterns that result from the cross-correlation of each pair of the ten linear arrays. A least squares inversion of the set of all such interference patterns provides the synthesized antenna pattern at each point in the cross-track field of view. Examples of the antenna pattern are shown in Figure 4 for a beam steered to nadir, -60° from nadir, and -70° from nadir. In each case, a uniform aperture taper has been used. The beams centered at nadir and -60° have well behaved sidelobes. However, a grating lobe at $+70^\circ$ is evident when the beam is steered to -70° . To determine the full range

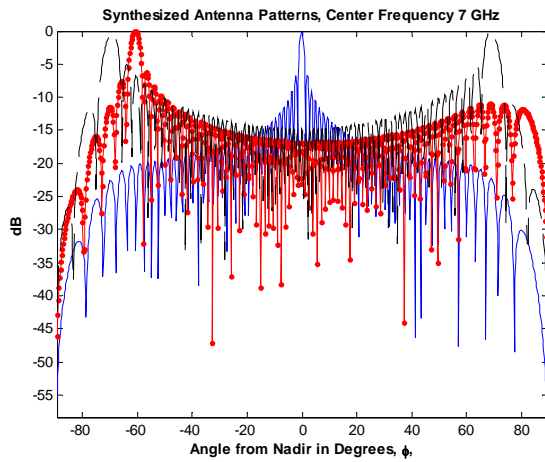


Figure 4. Synthesized antenna patterns at 7 GHz for a beam steered to nadir (blue), -60° from nadir (red) and -70° from nadir (black). Note the lack of grating lobes in the first two cases but the high grating lobe that appears at $+70^\circ$ in the third case.

of angles over which grating lobe-free beams can be formed, the beam efficiency is determined by numerical integration of the antenna pattern as its boresight angle is varied. The results are shown in Figure 5 using two different definitions of beam efficiency. The standard definition, in which the normalized pattern is integrated over the main beam, produces the dashed black curve in Fig.5. The beam efficiency at scan angles near nadir exceeds unity because of the negative sidelobes that are possible with a synthetic aperture radiometer. The solid blue curve in the figure uses an alternate definition, in which the square of the normalized pattern is integrated over the main beam. In this case, the beam efficiency cannot exceed unity. In both cases, there is a rapid drop in beam efficiency as the scan angle of the pattern exceeds 61° off nadir. This represents the onset of a significant grating lobe.

VI. SUMMARY

A synthetic thinned array radiometer design is presented which covers a 4-7 GHz frequency range. A planar antenna array is used with multi-resonant stacked microstrip patch radiating elements. The physical spacing between array elements in the scanning dimension is fixed at 0.9λ , which corresponds to $0.3-0.53\lambda$ over 4-7 GHz. The spacing, at 7 GHz, of greater than $\lambda/2$ necessitates a restriction of the off nadir scan angle to 61° or less.

The HIRad sensor provides push broom imagery of brightness temperature at the discrete frequencies of 4, 5, 6 and 7 GHz. From an aircraft altitude of 11 km, the spatial resolution of the image will be 0.9-1.4 km at nadir, with an $NE\Delta T$ of better than 0.3 K. The cross track swath width will be ± 20 km about the ground track. HIRad is expected to provide estimates in hurricanes of surface wind speed and rain rate that are comparable to those of the real aperture SFMR instrument at

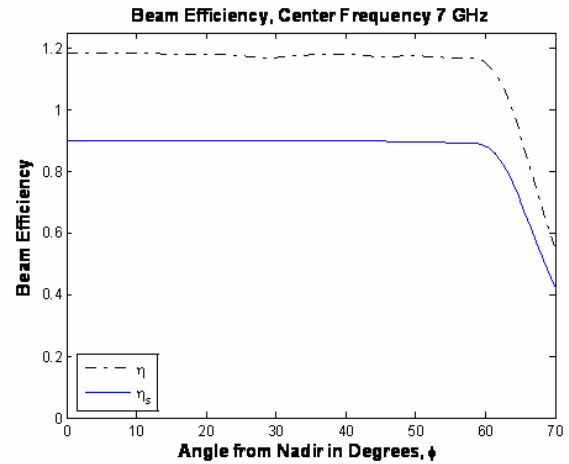


Figure 5. Beam efficiency of the synthesized antenna patterns at 7 GHz as a function of off-nadir boresight angle. The dashed black line assumes the standard definition for beam efficiency. The solid blue line integrates the square of the antenna pattern. In both cases, significant power begins to enter the grating lobe if the scan angle exceeds 61° away from nadir.

nadir, but with significantly improved spatial resolution. HIRad will also provide extended cross track coverage well beyond that of the nadir-only capabilities of SFMR. It is anticipated that the combination of extended coverage and improved spatial resolution will significantly improve upon SFMR's value as a tool for studying the internal structure of hurricanes and as a data source for operational hurricane forecasting models.

REFERENCES

- [1] Jones, W.L., P.G. Black, V.E. Delnore and C.T. Swift, "Airborne Microwave Remote Sensing Measurements of Hurricane Allen," *Science*, 214, 274-280, 1981.
- [2] Ruf, C., C. Principe, T. Dod, B. Gosselin, B. Monosmith, S. Musko, S. Rogacki, A. Stewart, Z. Zhang, "Lightweight Rainfall Radiometer STAR Aircraft Sensor," *Proc. IGARSS 2002, Toronto, CA, II: 850-852, 2002.*
- [3] Ruf, C. and C. Principe, "X-Band Lightweight Rainfall Radiometer First Light," *Proc. IGARSS 2003, Toulouse, FRANCE, 21-25 July 2003.*
- [4] Ruf, C.S., C.T. Swift, A.B. Tanner and D.M. Le Vine, "Interferometric synthetic aperture microwave radiometry for the remote sensing of the earth," *IEEE Trans. Geosci. Remote Sens.*, 26(5), 597-611, 1988.
- [5] Brown, S.T., and C.S. Ruf, "Validation and Development of Melting Layer Models Using Constraints by Active/Passive Microwave Observations of Rain and the Wind Roughened Ocean Surface," *AMS J. Oceanic Atmos. Tech.*, 24(4), 543-563, 2007.
- [6] Jones, W.L., J.-D. Park, J. Zec, C.S. Ruf, M.C. Bailey and J.W. Johnson, "A Feasibility Study for a Wide-Swath, Airborne, Hurricane Imaging Microwave Radiometer for Operational Hurricane Measurements," *Proc. IGARSS 2002, Toronto, CA, 24-28 June 2002.*
- [7] Ruf, C.S., "Numerical annealing of low redundancy linear arrays," *IEEE Trans. Antennas and Propag.*, 41(1), 85-90, 1993.
- [8] Ruf, C.S., S. M. Gross and S. Misra, "RFI Detection and Mitigation for Microwave Radiometry with an Agile Digital Detector," *IEEE Trans. Geosci. Remote Sens.*, 44(3), 694-706, 2006.